


Disorder-free localization as a purely classical effectPablo Sala^{1,2,3,*}, Giuliano Giudici^{4,5,†} and Jad C. Halimeh^{4,5,‡}¹*Department of Physics and Institute for Quantum Information and Matter, California Institute of Technology, Pasadena, California 91125, USA*²*Walter Burke Institute for Theoretical Physics, California Institute of Technology, Pasadena, California 91125, USA*³*Department of Physics, Technische Universität München, James-Franck-Straße 1, D-85748 Garching, Germany*⁴*Department of Physics and Arnold Sommerfeld Center for Theoretical Physics (ASC), Ludwig-Maximilians-Universität München, Theresienstraße 37, D-80333 München, Germany*⁵*Munich Center for Quantum Science and Technology (MCQST), Schellingstraße 4, D-80799 München, Germany* (Received 22 March 2023; revised 31 January 2024; accepted 31 January 2024; published 28 February 2024)

Disorder-free localization (DFL) is an ergodicity-breaking mechanism that has been shown to occur in lattice gauge theories in the quench dynamics of initial states spanning an extensive number of gauge superselection sectors. Whether this type of DFL is intrinsically a quantum interference effect or can arise classically has hitherto remained an open question whose resolution is pertinent to further understanding the far-from-equilibrium dynamics of gauge theories. In this work, we utilize cellular automaton circuits to model the quench dynamics of large-scale quantum link model (QLM) formulations of $(1 + 1)$ D quantum electrodynamics, showing excellent agreement with the exact quantum case for small system sizes. Our results demonstrate that DFL persists in the thermodynamic limit as a purely classical effect arising from the finite-size regularization of the gauge-field operator in the QLM formulation, and that quantum interference, though not a necessary condition, may be employed to enhance DFL.

DOI: [10.1103/PhysRevB.109.L060305](https://doi.org/10.1103/PhysRevB.109.L060305)

Introduction. The pursuit of a general theoretical framework of the nonequilibrium dynamics of quantum many-body systems is a major goal in condensed matter physics [1–4]. Whereas generic interacting many-body models are expected to thermalize according to the eigenstate thermalization hypothesis (ETH) [5,6], it has become clear that several ETH violations exist. Examples include integrable systems [7], systems with quantum many-body scars [8,9], Hilbert space fragmentation [10,11], and many-body localization (MBL) [12–16]. The latter was first predicted to exist in disordered systems. However, it is now known that the presence of disorder is not a necessary ingredient, and without it, localization can still arise. For example, so-called Stark MBL involves adding a strong tilted potential in a clean system of interacting fermions [17,18], which has also been experimentally demonstrated to lead to strong suppression of the dynamics in cold-atom and trapped-ion quantum simulators [19,20]. Another mechanism for generating MBL without disorder appears in models with local constraints, known as gauge theories, which are fundamental frameworks of modern physics that describe the interactions of elementary particles as mediated by gauge bosons [21,22]. The principal property of gauge theories is their *local gauge invariance*, which encodes the laws of nature through intrinsic relations between the local distribution of matter and the surrounding electric

fields, as exemplified through Gauss’s law in quantum electrodynamics (QED). Upon preparing the system in a linear combination of an extensive number of gauge superselection sectors and subsequently performing a global quench, localized dynamics can emerge where the system retains memory of its initial state [23,24]. This appears to occur even when the quench Hamiltonian is nonintegrable, disorder-free, and translation-invariant with a homogeneous initial state. This ergodicity-breaking mechanism, known as *disorder-free localization* (DFL), has been demonstrated in various models [25–38], and has generally been attributed to an emergent effective disorder associated with the background charges corresponding to the spanned gauge superselection sectors.

In Brenes *et al.* [24], DFL was studied in the Schwinger model, where Gauss’s law was employed to integrate out the gauge fields, resulting in a purely fermionic model with long-range Coulomb interactions and an explicit correlated-disorder term related to the background charges. Soon thereafter, it was shown that DFL also persists, at least for small system sizes, at zero gauge coupling for *quantum link model* (QLM) regularizations of the Schwinger model, where the gauge and electric-field operators are represented by spin- S operators [39]. Lattice QED is then approached in the limit $S \rightarrow \infty$, although the low-energy physics is faithfully reproduced already for small values of S [40,41]. Interestingly, it was recently shown that starting in thermal ensembles spanning an extensive number of gauge superselection sectors, quench dynamics can give rise to DFL in QLMs and in \mathbb{Z}_2 gauge theories [42]. These works suggest that DFL can occur without explicit disorder and perhaps without the need of

*psala@caltech.edu

†giuliano.giudici@physik.uni-muenchen.de

‡jad.halimeh@physik.lmu.de

quantum interference. This has raised the question as to the origin of DFL. The fact that quantum simulation of gauge theories has recently become a very active research area in quantum many-body physics, and experimental realizations abound [43–57], motivates a better theoretical understanding of exotic nonergodic gauge-theory dynamics that can be probed on such platforms.

In this work, we ask whether DFL in lattice gauge theories can arise *purely classically*, i.e., in the absence of any quantum interference effect. We approach this question by modeling the dynamics of spin- S $U(1)$ QLMs using cellular automaton circuits (CACs), which have been employed in several recent works on systems with unconventional symmetries [58–66]. Here we show that DFL persists in the thermodynamic limit as a purely classical effect. We attribute this form of DFL to the regularized *finite* structure of gauge superselection sectors in QLMs, leading to reducible dynamics as in systems showcasing Hilbert space fragmentation, here explicitly given by the local gauge invariance [10,11,67–69]. Furthermore, we show excellent quantitative agreement of the saturation values of the imbalance and infinite-temperature correlations with the quantum case through exact diagonalization (ED) on small system sizes. We argue that this type of DFL is distinct from, though can occur concomitantly with, the type connected to a finite gauge coupling in the Schwinger model.

Cellular automaton circuits. In a QLM, the matter and gauge degrees of freedom are represented by a spin-1/2 variable $\hat{\sigma}_j^\alpha$ and a spin- S variable $\hat{s}_{j,j+1}^\alpha$, respectively. Here $j = 1, \dots, L$ labels the sites of a chain of length L with periodic boundary conditions and $\alpha = x, y, z$ is the spin component. The matter fields live on the sites, and the gauge variables, i.e., the discretized local electric field, live on the links between two sites. The states of the computational basis are the strings $C = (\sigma_1^z, s_{1,2}^z, \sigma_2^z, \dots, s_{L-1,L}^z, \sigma_L^z, s_{L,1}^z)$, where $\sigma_j^z \in \{-1, +1\}$ and $s_{j,j+1}^z \in \{-S, \dots, S\}$. The standard QLM dynamics, which we will introduce later, commutes with the Gauss's law operator

$$\hat{G}_j = (-1)^j [\hat{s}_{j-1,j}^z + \hat{s}_{j,j+1}^z + (\hat{\sigma}_j^z + \mathbb{1})/2]. \quad (1)$$

Since this operator is diagonal, gauge invariance can be encoded into a classical cellular automaton, namely a particular kind of dynamics which maps computational basis states into computational basis states. In this setting, the quantum spins are demoted to classical variables σ_j and $s_{j,j+1}$, and the state of the system at any time t is given by a string configuration $C(t)$. The conservation law (1) is enforced by only allowing symmetric updates of this string. A similar approach has been employed to probe the hydrodynamic behavior of classical systems with kinetic constraints and different kinds of unconventional conservation laws such as dipole-moment conservation [58–66].

The dynamics of the classical CAC considered here is schematically depicted in Fig. 1(a): local gates $P_{j,j+1}$ act on pairs of neighboring sites ($j, j+1$) and their intermediate link, and the matter and gauge degrees of freedom are updated as $\sigma_j \rightarrow \sigma_j \pm 2$, $\sigma_{j+1} \rightarrow \sigma_{j+1} \pm 2$, and $s_{j,j+1} \rightarrow s_{j,j+1} \mp 1$, respectively. These updates are randomly applied among those for which $|\sigma_j \pm 2| = 1$, $|\sigma_{j+1} \pm 2| = 1$, and $|s_{j,j+1} \pm 1| \leq S$, with symmetric transition rates such that detailed balance is satisfied on the uniformly random ensemble of string

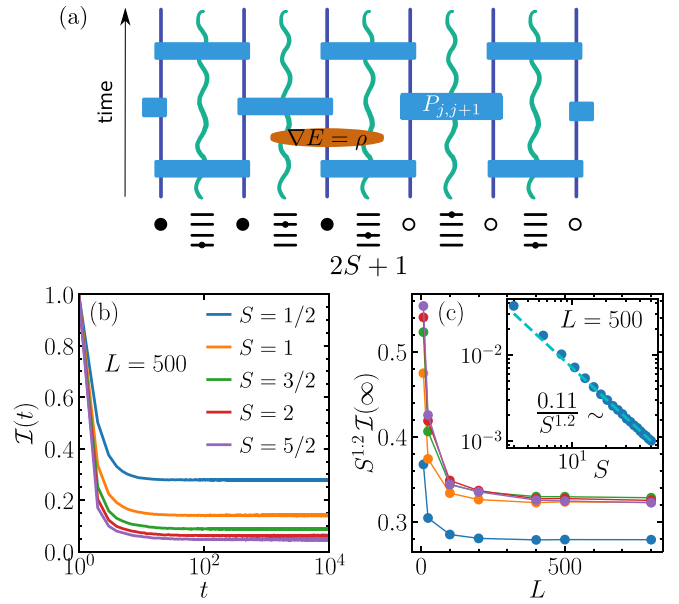


FIG. 1. Disorder-free localization as a purely classical effect. (a) Schematic of the cellular automaton implementation of the spin- S $U(1)$ QLM (3) and the enforcement of Gauss's law. Purple straight lines and green wiggly lines indicate the discrete time evolution of matter sites and gauge links, respectively. A matter site is either empty (\circ) or occupied (\bullet), while the electric field takes on values in $\{-S, \dots, S\}$. (b) Dynamics of the imbalance starting in a domain-wall state of $L = 500$ sites and averaging over $N = 8000$ randomly chosen electric-field configurations, modeling a superposition of an extensive number of gauge superselection sectors in the quantum case. Disorder-free localization arises for all considered values of S . Throughout this Letter, we have used $N = 10000$ for system sizes $L < 200$ and $N = 8000$ for $L \geq 200$. (c) Infinite-time value of the imbalance shows convergence with system size for $L \gtrsim 400$, indicating persistence in the thermodynamic limit with a power-law behavior in S , as shown in the inset.

configurations C . As a result, a local gate $P_{j,j+1}$ simply implements a random permutation between two allowed strings $C \rightarrow P_{j,j+1}C$. A time step is then given by a sequence of such non-overlapping gates acting on neighboring sites and the links in between, as shown in Fig. 1(a). The full time evolution follows from the application of several such layers of gates.

One can see that $G_j(P_{i,i+1}C) = G_j(C)$ for any configuration C and for all $i, j = 1, \dots, L$. This is trivially true for $i \neq j-1, j$. In the remainder cases, one finds $G_j(P_{i,i+1}C) = G_j(C) \pm (1-2\frac{1}{2}) = G_j(C)$. Hence, the CAC introduced above leaves G_j invariant for all j and at all times. Its eigenvalues g_j are the so-called background charges, and $(-1)^j g_j$ are integers in $\{-2S, \dots, 2S+1\}$. Gauge superselection sectors $\mathcal{C}_{\mathbf{g}}$ are defined as unique sets of these eigenvalues $\mathbf{g} = \{g_1, g_2, \dots, g_L\}$. It is worth noting here that not all charge configurations are physical, and, as we will see later, this truncation of the gauge and electric fields will have consequences on DFL that get more pronounced with smaller S . Overall, this leads to reducible classical dynamics whose sectors correspond exactly to the gauge superselection sectors of the spin- S QLM. This motivates us to investigate whether DFL,

well-established for the QLM, can also arise in this *purely classical* setting.

Localized dynamics from CAC. We now probe DFL in the CAC dynamics outlined above by computing the long-time saturation value of two different quantities: (i) the matter imbalance $\mathcal{I}(t) = \sum_{j=1}^L \langle \hat{\sigma}_j^z(0) \rangle \langle \hat{\sigma}_j^z(t) \rangle / L$, and (ii) the two-point unequal-time matter correlation function $\langle \hat{\sigma}_j^z(t) \hat{\sigma}_0^z(0) \rangle$. Both (i) and (ii) rely on the calculation of diagonal observables, and can thus be computed in the classical CAC framework by simply replacing $\hat{\sigma}_j^z$ with the classical variable σ_j . The expectation value $\langle A \rangle$ for a diagonal observable A corresponds to the average over N different initial conditions $C(0)$: $\langle A(t) \rangle \equiv \sum_{\{C(t)\}} A[C(t)] / N$. For (i), we prepare initial strings $C(0)$ with a domain-wall structure in the matter degrees of freedom, i.e., $\sigma_j(0) = \pm 1$ on the left (right) half of the chain, and a uniform random configuration of the electric field variables $s_{j,j+1}$. For (ii), instead, both matter and gauge fields are initialized randomly. In the following, we refer to random initial conditions as “infinite temperature.”

The imbalance dynamics (i) is shown in Fig. 1(b) for a system of $L = 500$ and $N = 8000$ for various values of S . The imbalance settles into a plateau at intermediate times that persists for all investigated timescales ($t \leq 10^4$ time steps), indicating clear features of DFL. These results can be considered to be in the thermodynamic limit, as shown by the finite-size scaling of the plateau value of $\mathcal{I}(t)$ in Fig. 1(c), which demonstrates convergence with system size for $L \gtrsim 400$ at all considered values of S . The plateau also exhibits a power-law decay with S at sufficiently large S , as shown in the inset of Fig. 1(c) for $L = 500$, indicating a vanishing value in the limit $S \rightarrow \infty$.

We now turn to the computation of the matter two-time correlation function (ii) $\langle \sigma_j(t) \sigma_0(0) \rangle$, where we initialize the circuit in a state with both matter and gauge degrees of freedom at infinite temperature. The discrete dynamics of the equal-space ($j = 0$) two-time function for $S = 1/2$ and $S = 1$ is plotted for various values of L , indicating convergence to the thermodynamic limit as shown in Figs. 2(a) and 2(b). Its long-time value is shown in Fig. 2(c) for L up to 400 sites as a function of S . The saturation value attained by the correlation function for $t \rightarrow \infty$ can be lower-bounded by making use of the conserved quantities via Mazur’s bound M_S [70]. Such a bound holds for both quantum and classical systems as long as the correlation function is evaluated on stationary states of the dynamics [70,71] and the same set of conserved quantities is considered. Generically, this bound vanishes in the thermodynamic limit for standard conserved quantities like e.g., particle number. However, for the Gauss’s law Eq. (1) it leads to the finite value $M_S = 3/[4S(S+1)]$ for any finite S [72]. We can improve this bound by taking the projectors $\hat{P}_{\mathbf{g}}$ onto the superselection sectors $C_{\mathbf{g}}$ labeled by the background-charge distribution \mathbf{g} as conserved quantities, yielding

$$\lim_{T \rightarrow \infty} \frac{1}{T} \int_0^T dt \langle \sigma_0(t) \sigma_0(0) \rangle \geq \sum_{\mathbf{g}} \frac{\text{Tr}\{\sigma_0 \hat{P}_{\mathbf{g}}\}^2}{\text{Tr}\{\hat{P}_{\mathbf{g}}\}} \equiv M_S, \quad (2)$$

where $\text{Tr}\{\hat{A} \hat{P}_{\mathbf{g}}\} \equiv \sum_{C \in C_{\mathbf{g}}} A(C)$. The same approach was used to show a finite saturation value of infinite-temperature correlations in the presence of strong fragmentation of the Hilbert space [10], as well as for boundary correlations [66,73,74].

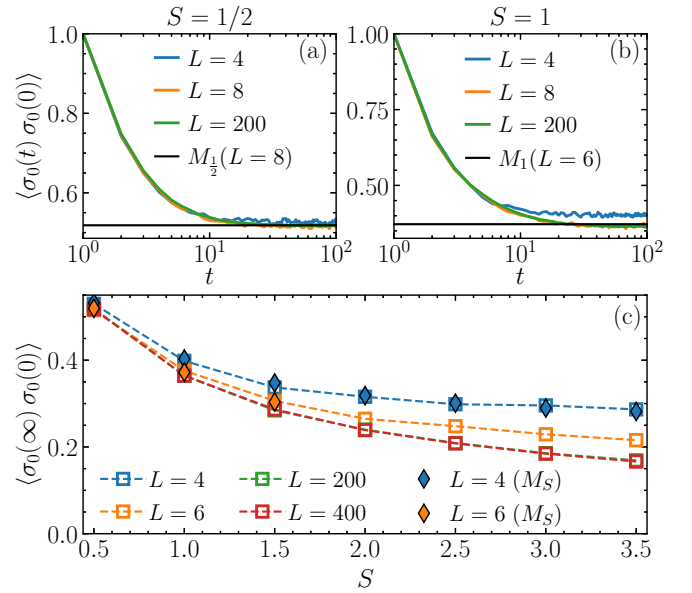


FIG. 2. Localized dynamics of the matter autocorrelator. Modeling of the dynamics of the matter autocorrelator for (a) $S = 1/2$ and (b) $S = 1$, using cellular automaton circuits. The black horizontal line demarcates the corresponding Mazur bound (2). (c) Infinite-time value of the matter autocorrelator, showing a monotonic decrease with S , and convergence to the thermodynamic limit for system sizes $L \gtrsim 200$ sites. Diamonds represent the finite-size Mazur’s bounds obtained from Eq. (2).

In practice, we numerically compute M_S by scanning over all superselection sectors. We observe that its value mildly depends on the system size L and provides a tight bound on equal-space two-time correlations, as shown in Fig. 2. We also note that the saturation value scales as $S^{-0.66}$ [72].

Comparison to DFL in QLM. We now compare the CAC results to those obtained from exact diagonalization for the quantum dynamics. The spin- S quantum link model Hamiltonian [75–78] takes the form

$$\hat{H} = \sum_{j=1}^L \left[\frac{J}{2\sqrt{S(S+1)}} (\hat{\sigma}_j^- \hat{s}_{j,j+1}^+ \hat{\sigma}_{j+1}^- + \text{H.c.}) + \frac{\mu}{2} \hat{\sigma}_j^z + \frac{\kappa^2}{2} (\hat{s}_{j,j+1}^z)^2 \right], \quad (3)$$

where $\hat{\sigma}_j^\alpha$ and $\hat{s}_{j,j+1}^\alpha$, $\alpha = x, y, z$, are Pauli matrices and spin- S operators $\hat{s}_{j,j+1}^\alpha$, respectively, $\hat{\sigma}^\pm = \hat{\sigma}^x \pm i\hat{\sigma}^y$, and $\hat{s}^\pm = \hat{s}^x \pm i\hat{s}^y$. The coupling constant $J = 1$ sets the overall energy scale, μ is the mass of the matter particles, and κ is the gauge-coupling strength. The spin-1/2 formulation of Eq. (3) has been experimentally realized in large-scale implementations using Rydberg atoms [43,79] and tilted Bose–Hubbard superlattices [52,53,57]. The QLM Hamiltonian (3) hosts a $U(1)$ gauge invariance with generators given in Eq. (1).

We start comparing the results when $\mu = \kappa = 0$ in Eq. (3) for the two-point matter classical and quantum correlators, namely $\langle \sigma_j(t) \sigma_0(0) \rangle$ and $\langle \hat{\sigma}_j^z(t) \hat{\sigma}_0^z(0) \rangle = \text{Tr}[\hat{\sigma}_j^z(t) \hat{\sigma}_0^z(0)]$, respectively, for $t \rightarrow \infty$. These are shown in Fig. 3(a) for $L = 8$ sites and several values of S . For the computation of quantum correlators, we exploit dynamical typicality and obtain

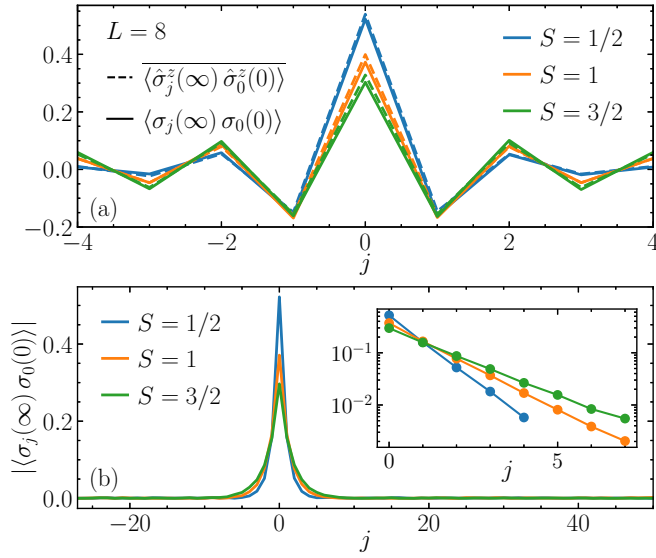


FIG. 3. Correlation spatial profile. (a) Spatial profile of the two-point unequal-time correlator at $t \rightarrow \infty$, obtained through CAC (ED) for the classical (quantum) case. For all considered values of S , we find excellent agreement between the classical and quantum cases. (b) Spatial profile of the two-point unequal-time correlator calculated from CAC at $t \rightarrow \infty$ for $L = 200$ sites, showing exponential localization for all considered values of S . The inset shows that localization is more prominent with decreasing S .

infinite temperature averages starting from random initial pure states [72,80]. We observe excellent agreement between the stationary states of the classical and quantum cases saturating to the common finite Mazur bound M_S for sufficiently large system sizes. Furthermore, we employ CAC to calculate the spatial profile for $L = 200$ sites and several values of S in Fig. 3(b), showing exponential localization in all considered cases. This quantitative agreement corroborates the equivalent propagation of local perturbations under CAC and quantum evolution at infinite temperature, which is halted due to the interplay of an extensive number of superselection sectors in the dynamics. Moreover, we note that the imbalance dynamics (i) approaches the same value for $t \rightarrow \infty$ in the classical CAC and quantum model (3) upon breaking energy conservation in the latter [72].

Given that the CAC computation is inherently classical, and yet we see DFL for all S , we are led to conclude that the occurrence of DFL in spin- S U(1) QLMs does not require quantum interference. Instead, it is in this case a purely classical effect that can be attributed to the regularized finite structure of gauge sectors at finite S . Indeed, Figs. 1(b) and 1(c) show that the imbalance plateau takes on a value that decreases with S , while Figs. 2(c) and 3(b) show that the peak in the long-time spatial profile of the matter two-time function is also a decreasing function of S . These observations indicate that in the limit of $S \rightarrow \infty$, DFL originating due to this classical effect is not expected to emerge.

We have found that the CAC computation employed here faithfully models the stationary state of the infinite-temperature correlation-function dynamics generated by the Hamiltonian (3) for $\mu = \kappa = 0$. In the lattice Schwinger

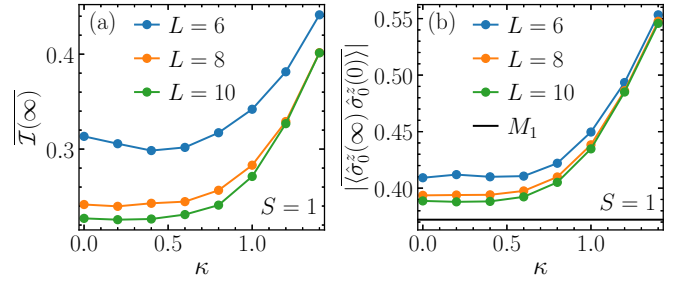


FIG. 4. Effect of gauge coupling. (a) Plateau value of the imbalance as a function of the gauge coupling κ for $S = 1$ in the quantum case, calculated in ED. At sufficiently large system size L , we find a monotonic increase with κ in the plateau value. (b) The equal-space two-time correlator at $t \rightarrow \infty$ as a function of κ as computed in ED for the quantum case. Similarly to the imbalance plateau, it shows a monotonic increase with κ at sufficiently large L . Mazur's bound M_1 is the black horizontal line.

model limit $S = \infty$, it was argued that a finite κ is a necessary condition for DFL to emerge [24]. We have shown that, for finite S , this is not the case, and the finite regularization of the gauge sectors in the spin- S QLM suffices for DFL to emerge.

We now study the effect of finite κ on DFL. For this purpose, we focus on $S = 1$ in Fig. 4 [81]. Using ED, we calculate the quench dynamics of the imbalance starting in an initial state with a domain-wall structure in the matter fields and gauge degrees of freedom at infinite temperature. We find that the plateau value of the imbalance [Fig. 4(a)] increases with κ from the saturation value at $\kappa = 0$. Similarly, the equal-space two-time correlator at $t \rightarrow \infty$ increases with κ [Fig. 4(b)]. This confirms the conclusion of Ref. [24] that κ acts as disorder strength enhancing the localization. However, we note that at finite S their mapping from the lattice Schwinger model to an interacting fermionic system with correlated disorder is no longer exact.

Discussion and outlook. Using CAC, we were able to show that DFL can arise in the spin- S U(1) QLM solely from the finite regularization of its gauge sectors, without the need for finite gauge coupling, which is necessary only for having DFL in the limit $S \rightarrow \infty$. We validated our conclusions by modeling the dynamics of the imbalance and infinite-temperature two-point unequal-time correlation functions, showing excellent agreement with results from the exact diagonalization of the full quantum model at small system sizes.

Since CAC is an inherently classical setup, our results show that quantum interference is not a necessary condition for localization when combining extensively many superselection sectors. This is related to other forms of localization in the absence of disorder, such as in the context of Hilbert space fragmentation. Since DFL has been established as an ergodicity-breaking paradigm in gauge theories, a thorough understanding of its origin can shed light on the nonequilibrium dynamics of such models.

An interesting avenue for future work would be to understand how prominent classical DFL is in higher dimension [82], and to explore the role of the emergent random potential in the Schwinger model in competition with the long-range

Coulomb potential [24]. It would be also interesting to understand the thermal properties of each of the involved superselection sectors, which combined lead to finite correlations, and investigate the specific constrained structure arising at finite S . In dipole-conserving systems, the cause of this behavior has been associated with the presence of statistically localized degrees of freedom that label all Krylov subspaces left invariant by the dynamics [73,83].

Acknowledgments. The authors are grateful to J. Knolle, J. Lehmann, Y. Li, F. Pollmann, T. Rakovszky, and F. Surace for enlightening discussions and for previous collaborations on related topics. This work was supported by the Walter Burke

Institute for Theoretical Physics at Caltech, and the Institute for Quantum Information and Matter. J.C.H. acknowledges funding from the European Research Council (ERC) under the European Union's Horizon 2020 research and innovation program (Grant Agreement No. 948141)–ERC Starting Grant SimUcQuam, and by the Deutsche Forschungsgemeinschaft (DFG, German Research Foundation) under Germany's Excellence Strategy, EXC-2111, 390814868. G.G. acknowledges support from the Deutsche Forschungsgemeinschaft (DFG, German Research Foundation) under Germany's Excellence Strategy, EXC-2111, 390814868, and from the ERC grant QSIMCORR, ERC-2018-COG, No. 771891.

-
- [1] J. Eisert, M. Friesdorf, and C. Gogolin, Quantum many-body systems out of equilibrium, *Nat. Phys.* **11**, 124 (2015).
- [2] L. D'Alessio, Y. Kafri, A. Polkovnikov, and M. Rigol, From quantum chaos and eigenstate thermalization to statistical mechanics and thermodynamics, *Adv. Phys.* **65**, 239 (2016).
- [3] J. M. Deutsch, Eigenstate thermalization hypothesis, *Rep. Prog. Phys.* **81**, 082001 (2018).
- [4] B. Buča, Unified theory of local quantum many-body dynamics: Eigenoperator thermalization theorems, *Phys. Rev. X* **13**, 031013 (2023).
- [5] J. M. Deutsch, Quantum statistical mechanics in a closed system, *Phys. Rev. A* **43**, 2046 (1991).
- [6] M. Srednicki, Chaos and quantum thermalization, *Phys. Rev. E* **50**, 888 (1994).
- [7] M. Rigol, V. Dunjko, and M. Olshanii, Thermalization and its mechanism for generic isolated quantum systems, *Nature (London)* **452**, 854 (2008).
- [8] S. Moudgalya, S. Rachel, B. A. Bernevig, and N. Regnault, Exact excited states of nonintegrable models, *Phys. Rev. B* **98**, 235155 (2018).
- [9] C. J. Turner, A. A. Michailidis, D. A. Abanin, M. Serbyn, and Z. Papić, Weak ergodicity breaking from quantum many-body scars, *Nat. Phys.* **14**, 745 (2018).
- [10] P. Sala, T. Rakovszky, R. Verresen, M. Knap, and F. Pollmann, Ergodicity breaking arising from Hilbert space fragmentation in dipole-conserving Hamiltonians, *Phys. Rev. X* **10**, 011047 (2020).
- [11] V. Khemani, M. Hermele, and R. Nandkishore, Localization from Hilbert space shattering: From theory to physical realizations, *Phys. Rev. B* **101**, 174204 (2020).
- [12] D. M. Basko, I. L. Aleiner, and B. L. Altshuler, Metal-insulator transition in a weakly interacting many-electron system with localized single-particle states, *Ann. Phys.* **321**, 1126 (2006).
- [13] I. V. Gornyi, A. D. Mirlin, and D. G. Polyakov, Interacting electrons in disordered wires: Anderson localization and low- T transport, *Phys. Rev. Lett.* **95**, 206603 (2005).
- [14] R. Nandkishore and D. A. Huse, Many-body localization and thermalization in quantum statistical mechanics, *Annu. Rev. Condens. Matter Phys.* **6**, 15 (2015).
- [15] D. A. Abanin, E. Altman, I. Bloch, and M. Serbyn, Colloquium: Many-body localization, thermalization, and entanglement, *Rev. Mod. Phys.* **91**, 021001 (2019).
- [16] F. Alet and N. Laflorencie, Many-body localization: An introduction and selected topics, *C. R. Phys.* **19**, 498 (2018).
- [17] E. van Nieuwenburg, Y. Baum, and G. Refael, From Bloch oscillations to many-body localization in clean interacting systems, *Proc. Natl. Acad. Sci. USA* **116**, 9269 (2019).
- [18] M. Schulz, C. A. Hooley, R. Moessner, and F. Pollmann, Stark many-body localization, *Phys. Rev. Lett.* **122**, 040606 (2019).
- [19] S. Scherg, T. Kohlert, P. Sala, F. Pollmann, B. Hebbes Madhusudhana, I. Bloch, and M. Aidelsburger, Observing non-ergodicity due to kinetic constraints in tilted Fermi-Hubbard chains, *Nat. Commun.* **12**, 4490 (2021).
- [20] W. Morong, F. Liu, P. Becker, K. S. Collins, L. Feng, A. Kyprianidis, G. Pagano, T. You, A. V. Gorshkov, and C. Monroe, Observation of Stark many-body localization without disorder, *Nature (London)* **599**, 393 (2021).
- [21] S. Weinberg, *The Quantum Theory of Fields, Vol. 2, Modern Applications* (Cambridge University Press, Cambridge, UK, 1995).
- [22] C. Gattringer and C. Lang, *Quantum Chromodynamics on the Lattice: An Introductory Presentation* (Springer, Berlin, 2009).
- [23] A. Smith, J. Knolle, D. L. Kovrizhin, and R. Moessner, Disorder-free localization, *Phys. Rev. Lett.* **118**, 266601 (2017).
- [24] M. Brenes, M. Dalmonte, M. Heyl, and A. Scardicchio, Many-body localization dynamics from gauge invariance, *Phys. Rev. Lett.* **120**, 030601 (2018).
- [25] A. Smith, J. Knolle, R. Moessner, and D. L. Kovrizhin, Absence of ergodicity without quenched disorder: From quantum disentangled liquids to many-body localization, *Phys. Rev. Lett.* **119**, 176601 (2017).
- [26] A. Metavitsiadis, A. Pidotella, and W. Brenig, Thermal transport in a two-dimensional \mathbb{Z}_2 spin liquid, *Phys. Rev. B* **96**, 205121 (2017).
- [27] A. Smith, J. Knolle, R. Moessner, and D. L. Kovrizhin, Dynamical localization in \mathbb{Z}_2 lattice gauge theories, *Phys. Rev. B* **97**, 245137 (2018).
- [28] J. Park, Y. Kuno, and I. Ichinose, Glassy dynamics from quark confinement: Atomic quantum simulation of the gauge-Higgs model on a lattice, *Phys. Rev. A* **100**, 013629 (2019).
- [29] A. Russomanno, S. Notarnicola, F. M. Surace, R. Fazio, M. Dalmonte, and M. Heyl, Homogeneous Floquet time crystal protected by gauge invariance, *Phys. Rev. Res.* **2**, 012003(R) (2020).
- [30] I. Papaefstathiou, A. Smith, and J. Knolle, Disorder-free localization in a simple $U(1)$ lattice gauge theory, *Phys. Rev. B* **102**, 165132 (2020).

- [31] P. A. McClarty, M. Haque, A. Sen, and J. Richter, Disorder-free localization and many-body quantum scars from magnetic frustration, *Phys. Rev. B* **102**, 224303 (2020).
- [32] O. Hart, S. Gopalakrishnan, and C. Castelnovo, Logarithmic entanglement growth from disorder-free localization in the two-leg compass ladder, *Phys. Rev. Lett.* **126**, 227202 (2021).
- [33] G.-Y. Zhu and M. Heyl, Subdiffusive dynamics and critical quantum correlations in a disorder-free localized Kitaev honeycomb model out of equilibrium, *Phys. Rev. Res.* **3**, L032069 (2021).
- [34] P. Karpov, R. Verdel, Y.-P. Huang, M. Schmitt, and M. Heyl, Disorder-free localization in an interacting 2D lattice gauge theory, *Phys. Rev. Lett.* **126**, 130401 (2021).
- [35] J. Sous, B. Kloss, D. M. Kennes, D. R. Reichman, and A. J. Millis, Phonon-induced disorder in dynamics of optically pumped metals from nonlinear electron-phonon coupling, *Nat. Commun.* **12**, 5803 (2021).
- [36] J. C. Halimeh, L. Homeier, H. Zhao, A. Bohrdt, F. Grusdt, P. Hauke, and J. Knolle, Enhancing disorder-free localization through dynamically emergent local symmetries, *PRX Quantum* **3**, 020345 (2022).
- [37] N. Chakraborty, M. Heyl, P. Karpov, and R. Moessner, Disorder-free localization transition in a two-dimensional lattice gauge theory, *Phys. Rev. B* **106**, L060308 (2022).
- [38] C. Gao, Z. Tang, F. Zhu, Y. Zhang, H. Pu, and L. Chen, Non-thermal dynamics in a spin- $\frac{1}{2}$ lattice Schwinger model, *Phys. Rev. B* **107**, 104302 (2023).
- [39] J. C. Halimeh, H. Zhao, P. Hauke, and J. Knolle, Stabilizing disorder-free localization, [arXiv:2111.02427](https://arxiv.org/abs/2111.02427).
- [40] T. V. Zache, M. Van Damme, J. C. Halimeh, P. Hauke, and D. Banerjee, Toward the continuum limit of a $(1+1)$ D quantum link Schwinger model, *Phys. Rev. D* **106**, L091502 (2022).
- [41] J. C. Halimeh, M. V. Damme, T. V. Zache, D. Banerjee, and P. Hauke, Achieving the quantum field theory limit in far-from-equilibrium quantum link models, *Quantum* **6**, 878 (2022).
- [42] J. C. Halimeh, P. Hauke, J. Knolle, and F. Grusdt, Temperature-induced disorder-free localization, [arXiv:2206.11273](https://arxiv.org/abs/2206.11273).
- [43] H. Bernien, S. Schwartz, A. Keesling, H. Levine, A. Omran, H. Pichler, S. Choi, A. S. Zibrov, M. Endres, M. Greiner, V. Vuletić, and M. D. Lukin, Probing many-body dynamics on a 51-atom quantum simulator, *Nature (London)* **551**, 579 (2017).
- [44] C. Kokail, C. Maier, R. van Bijnen, T. Brydges, M. K. Joshi, P. Jurcevic, C. A. Muschik, P. Silvi, R. Blatt, C. F. Roos, and P. Zoller, Self-verifying variational quantum simulation of lattice models, *Nature (London)* **569**, 355 (2019).
- [45] E. A. Martinez, C. A. Muschik, P. Schindler, D. Nigg, A. Erhard, M. Heyl, P. Hauke, M. Dalmonte, T. Monz, P. Zoller, and R. Blatt, Real-time dynamics of lattice gauge theories with a few-qubit quantum computer, *Nature (London)* **534**, 516 (2016).
- [46] C. Muschik, M. Heyl, E. Martinez, T. Monz, P. Schindler, B. Vogell, M. Dalmonte, P. Hauke, R. Blatt, and P. Zoller, U(1) Wilson lattice gauge theories in digital quantum simulators, *New J. Phys.* **19**, 103020 (2017).
- [47] N. Klco, E. F. Dumitrescu, A. J. McCaskey, T. D. Morris, R. C. Pooser, M. Sanz, E. Solano, P. Lougovski, and M. J. Savage, Quantum-classical computation of Schwinger model dynamics using quantum computers, *Phys. Rev. A* **98**, 032331 (2018).
- [48] C. Schweizer, F. Grusdt, M. Berngruber, L. Barbiero, E. Demler, N. Goldman, I. Bloch, and M. Aidelsburger, Floquet approach to \mathbb{Z}_2 lattice gauge theories with ultracold atoms in optical lattices, *Nat. Phys.* **15**, 1168 (2019).
- [49] F. Görg, K. Sandholzer, J. Minguzzi, R. Desbuquois, M. Messer, and T. Esslinger, Realization of density-dependent Peierls phases to engineer quantized gauge fields coupled to ultracold matter, *Nat. Phys.* **15**, 1161 (2019).
- [50] A. Mil, T. V. Zache, A. Hegde, A. Xia, R. P. Bhatt, M. K. Oberthaler, P. Hauke, J. Berges, and F. Jendrzejewski, A scalable realization of local U(1) gauge invariance in cold atomic mixtures, *Science* **367**, 1128 (2020).
- [51] N. Klco, M. J. Savage, and J. R. Stryker, SU(2) non-Abelian gauge field theory in one dimension on digital quantum computers, *Phys. Rev. D* **101**, 074512 (2020).
- [52] B. Yang, H. Sun, R. Ott, H.-Y. Wang, T. V. Zache, J. C. Halimeh, Z.-S. Yuan, P. Hauke, and J.-W. Pan, Observation of gauge invariance in a 71-site Bose-Hubbard quantum simulator, *Nature (London)* **587**, 392 (2020).
- [53] Z.-Y. Zhou, G.-X. Su, J. C. Halimeh, R. Ott, H. Sun, P. Hauke, B. Yang, Z.-S. Yuan, J. Berges, and J.-W. Pan, Thermalization dynamics of a gauge theory on a quantum simulator, *Science* **377**, 311 (2022).
- [54] N. H. Nguyen, M. C. Tran, Y. Zhu, A. M. Green, C. H. Alderete, Z. Davoudi, and N. M. Linke, Digital quantum simulation of the Schwinger model and symmetry protection with trapped ions, [arXiv:2112.14262](https://arxiv.org/abs/2112.14262).
- [55] Z. Wang, Z.-Y. Ge, Z. Xiang, X. Song, R.-Z. Huang, P. Song, X.-Y. Guo, L. Su, K. Xu, D. Zheng, and H. Fan, Observation of emergent \mathbb{Z}_2 gauge invariance in a superconducting circuit, *Phys. Rev. Res.* **4**, L022060 (2022).
- [56] J. Mildnerberger, W. Mruczkiewicz, J. C. Halimeh, Z. Jiang, and P. Hauke, Probing confinement in a \mathbb{Z}_2 lattice gauge theory on a quantum computer, [arXiv:2203.08905](https://arxiv.org/abs/2203.08905).
- [57] H.-Y. Wang, W.-Y. Zhang, Z.-Y. Yao, Y. Liu, Z.-H. Zhu, Y.-G. Zheng, X.-K. Wang, H. Zhai, Z.-S. Yuan, and J.-W. Pan, Interrelated thermalization and quantum criticality in a lattice gauge simulator, *Phys. Rev. Lett.* **131**, 050401 (2023).
- [58] J. Iaconis, S. Vijay, and R. Nandkishore, Anomalous subdiffusion from subsystem symmetries, *Phys. Rev. B* **100**, 214301 (2019).
- [59] J. Feldmeier, P. Sala, G. De Tomasi, F. Pollmann, and M. Knap, Anomalous diffusion in dipole- and higher-moment-conserving systems, *Phys. Rev. Lett.* **125**, 245303 (2020).
- [60] A. Morningstar, V. Khemani, and D. A. Huse, Kinetically constrained freezing transition in a dipole-conserving system, *Phys. Rev. B* **101**, 214205 (2020).
- [61] J. Iaconis, A. Lucas, and R. Nandkishore, Multipole conservation laws and subdiffusion in any dimension, *Phys. Rev. E* **103**, 022142 (2021).
- [62] O. Hart, A. Lucas, and R. Nandkishore, Hidden quasiconservation laws in fracton hydrodynamics, *Phys. Rev. E* **105**, 044103 (2022).
- [63] P. Patil, M. Heyl, and F. Alet, Anomalous relaxation of density waves in a ring-exchange system, *Phys. Rev. E* **107**, 034119 (2023).
- [64] P. Brighi, M. Ljubotina, and M. Serbyn, Hilbert space fragmentation and slow dynamics in particle-conserving quantum East models, *SciPost Phys.* **15**, 093 (2023).
- [65] J. Feldmeier, W. Witczak-Krempa, and M. Knap, Emergent tracer dynamics in constrained quantum systems, *Phys. Rev. B* **106**, 094303 (2022).

- [66] P. Sala, J. Lehmann, T. Rakovszky, and F. Pollmann, Dynamics in systems with modulated symmetries, [arXiv:2110.08302](https://arxiv.org/abs/2110.08302).
- [67] F. Ritort and P. Sollich, Glassy dynamics of kinetically constrained models, *Adv. Phys.* **52**, 219 (2003).
- [68] J. P. Garrahan, Aspects of non-equilibrium in classical and quantum systems: Slow relaxation and glasses, dynamical large deviations, quantum non-ergodicity, and open quantum dynamics, *Physica A* **504**, 130 (2018).
- [69] S. Moudgalya, B. A. Bernevig, and N. Regnault, Quantum many-body scars and Hilbert space fragmentation: A review of exact results, *Rep. Prog. Phys.* **85**, 086501 (2022).
- [70] P. Mazur, Non-ergodicity of phase functions in certain systems, *Physica* **43**, 533 (1969).
- [71] A. Dhar, A. Kundu, and K. Saito, Revisiting the Mazur bound and the Suzuki equality, *Chaos, Solitons Fractals* **144**, 110618 (2021).
- [72] See Supplemental Material at <http://link.aps.org/supplemental/10.1103/PhysRevB.109.L060305> for the Supplemental Material includes a discussion of Mazur's bound for our model, details on the numerical simulations, and a comparison of CAC and non-Hamiltonian dynamics, which includes Refs. [84,85].
- [73] T. Rakovszky, P. Sala, R. Verresen, M. Knap, and F. Pollmann, Statistical localization: From strong fragmentation to strong edge modes, *Phys. Rev. B* **101**, 125126 (2020).
- [74] J. Lehmann, P. Sala, F. Pollmann, and T. Rakovszky, Fragmentation-induced localization and boundary charges in dimensions two and above, [arXiv:2208.12260](https://arxiv.org/abs/2208.12260).
- [75] S. Chandrasekharan and U.-J. Wiese, Quantum link models: A discrete approach to gauge theories, *Nucl. Phys. B* **492**, 455 (1997).
- [76] U.-J. Wiese, Ultracold quantum gases and lattice systems: Quantum simulation of lattice gauge theories, *Ann. Phys.* **525**, 777 (2013).
- [77] V. Kasper, F. Hebenstreit, F. Jendrzejewski, M. K. Oberthaler, and J. Berges, Implementing quantum electrodynamics with ultracold atomic systems, *New J. Phys.* **19**, 023030 (2017).
- [78] P. Hauke, D. Marcos, M. Dalmonte, and P. Zoller, Quantum simulation of a lattice Schwinger model in a chain of trapped ions, *Phys. Rev. X* **3**, 041018 (2013).
- [79] F. M. Surace, P. P. Mazza, G. Giudici, A. Lerose, A. Gambassi, and M. Dalmonte, Lattice gauge theories and string dynamics in Rydberg atom quantum simulators, *Phys. Rev. X* **10**, 021041 (2020).
- [80] R. Steinigeweg, F. Jin, D. Schmidtke, H. De Raedt, K. Michielsen, and J. Gemmer, Real-time broadening of nonequilibrium density profiles and the role of the specific initial-state realization, *Phys. Rev. B* **95**, 035155 (2017).
- [81] For $S = 1/2$, the gauge-coupling term is an inconsequential energetic constant.
- [82] J. Osborne, I. P. McCulloch, and J. C. Halimeh, Disorder-free localization in $2 + 1$ D lattice gauge theories with dynamical matter, [arXiv:2301.07720](https://arxiv.org/abs/2301.07720).
- [83] S. Moudgalya and O. I. Motrunich, Hilbert space fragmentation and commutant algebras, *Phys. Rev. X* **12**, 011050 (2022).
- [84] M. Suzuki, Ergodicity, constants of motion, and bounds for susceptibilities, *Physica* **51**, 277 (1971).
- [85] J.-S. Caux and J. Mossel, Remarks on the notion of quantum integrability, *J. Stat. Mech.: Theory Exp.* (2011) P02023.